ORIGINAL RESEARCH ARTICLE

Seasonal pattern of the chlorophyll-*a* in a coastal lagoon from the southern Baja California (Mexico), described with *in situ* observations and MODIS-Aqua imagery

María del Carmen Jiménez-Quiroz[a],*, Raúl Martell-Dubois[b], Rafael Cervantes-Duarte[c], Sergio Cerdeira-Estrada[b]

[a] General Directorate for Fisheries Research in the Pacific, National Institute of Fisheries and Aquaculture, Del Carmen, Coyoacán, Mexico City, Mexico
[b] National Commission for the Knowledge and Use of Biodiversity (CONABIO), Mexico City, Mexico
[c] National Polytechnic Institute, Interdisciplinary Center of Marine Sciences, La Paz, Mexico

Abstract   This study aims to estimate, with a climatology perspective, the average seasonal pattern of phytoplankton biomass (SP-PBavg) and its distribution in Bahia Magdalena (Mexico) as a baseline to evaluate PB changes in future studies. This lagoon is in a semi-arid region, lacks river discharges, and channels with vegetation are limited at the north and south zones. SP-PBavg was estimated with chlorophyll-*a* (chl-*a*) data obtained in 21 sites on daily MODIS-Aqua imagery (2002—2013; n = 2,418) from a ready-to-use public database. The first step was to establish criteria to use imagery and validate with *in situ* observations taken in 14 sites (2002—2011; n = 312). MODIS-Aqua overestimated chl-*a* (mean $\pm$ confidence interval$_{95}$: 5.09 $\pm$ 0.97 mg m^{-3}; n = 225); with differences among sites. There were no differences near the inlet lagoon (p <0.05), where the water characteristics are Case-1 while values were significantly higher in the eastern shore and two or three times higher in the mouth of north and south

* Corresponding author at: Dirección General Adjunta de Investigación Pesquera en el Pacífico, Instituto Nacional de Pesca y Acuacultura, Secretaría de Agricultura y Desarrollo Rural, Av. México 190, Del Carmen, Coyoacán, 04100, Mexico City, Mexico.
E-mail addresses: carmen.jquiroz@inapesca.gob.mx (M. del Carmen Jiménez-Quiroz), rmartell@conabio.gob.mx (R. Martell-Dubois), scerdeira@conabio.gob.mx (S. Cerdeira-Estrada).

Production and hosting by Elsevier

channels, whose water characteristics are similar to Case-2. Multivariate statistical methods allow defining zones into the lagoon and describe their SP-PBavg with both *in situ* and MODIS Aqua data, but the former's sample size was small, and the patterns were only delineated. In the inlet surroundings, chl-*a* peaks from March/April to June/July. On the eastern shore, where MODIS Aqua and *in situ* data were correlated, despite concentration differences, chl-*a* is higher from March/April to October, with peaks in June and September. In the mouth of internal channels, chl-*a* was higher than other sites and during a longer period; however, the very high MODIS-Aqua values suggest that the satellite also detects organic matter supplied by phytoplankton and other vegetables, which explain the high lagoon's productivity. These results validate the use of MODIS Aqua imagery to describe the chl-*a* seasonal patterns in the sea's vicinity.

1. Introduction

The abundance and distribution of phytoplankton, one of the most important primary producers in coastal lagoons (Cloern et al., 2014; de La Lanza-Espino, 1994), depends on environmental and biological factors (Behrenfeld and Boss, 2014). In the subtropical region, particularly in up-welling areas, phytoplankton biomass (PB) follows seasonal patterns (SP) driven by the fertilization mechanisms, temperature, and lighting variability, among other factors. Short- and medium-term climate fluctuations, such as the El Niño − The Southern Oscillation (ENSO), also modify the phytoplankton phenology on both intra-annual and inter-annual scale (Jiménez-Quiroz et al., 2019). On the other hand, interactions of microalgae with other organisms are complex (Behrenfeld and Boss, 2014), and their abundance and taxonomic composition changes influence the structure of the trophic web (Coupel et al., 2015; Franco-Gordo et al., 2004; Sommer et al., 2002) including fishery resources. (Lynam et al., 2017).

Bahia Magdalena is the largest coastal lagoon in the Mexican Pacific; it is on the Baja California southwestern coast, a semi-arid region with no permanent fluvial drainages (Funes-Rodríguez et al., 2007). Its productivity depends on the wind-driven coastal upwellings, which are more frequent in spring and autumn (Zaytsev et al., 2003), and on the California Current's nutrient supply. This lagoon is responsible for a high proportion of the Baja California Sur fishery production (Cota-Nieto et al., 2015); however, the catch of some resources has wide variations among the years (García-Borbón, 2019), probably due to environmental and productivity changes, including phytoplankton phenology, abundance, and composition. From 2015 to 2017, global warming, together with the co-occurrence of the strongly positive temperature anomalies of the marine heatwave The Blob (2013−2015) in the northeastern Pacific (Bond et al., 2015) and the 2015−2016 ENSO, altered the composition and seasonal pattern of phytoplankton biomass (SP-PB) in Bahia Magdalena (Jiménez-Quiroz et al., 2019). These changes coincided with the abating of several mollusk abundances, which led to the closure of its fisheries with significant social consequences.

To identify the magnitude of the SP-PB changes is necessary to establish a baseline (hereafter SP-PBavg) or climatology, which represents the average conditions of

a time series (World Meteorological Organization, 2017). Gárate Lizárraga and Siqueiros-Beltrones (1998) suggested that the SP-PBavg in Bahia Magdalena is bimodal, as in other subtropical coastal lagoons, because the cell density increased significantly in spring (average 1982−1986: 277×10^3 cells l^{-1}) and autumn-winter (avg. 1982−1986: 330×10^3 cells l^{-1}). However, this pattern was based on monthly samplings carried out discontinuously, and without considering the tide's amplitude, between 1982 and 1986; on the other hand, the environment and biological communities changed significantly due to the strong 1982−1983 ENSO (Chavez et al., 2002). So, it is necessary to expand the sample size and use a more accessible indicator than cell counts.

Chlorophyll-*a* (chl-*a*) is an indicator of phytoplankton biomass (Behrenfeld and Boss, 2014; Boyer et al., 2009) despite the high variability of the chl-*a*: carbon rate in phytoplankton (Geider, 1987). Chl-*a* is evaluated at the site of interest or in water samples (hereafter referred to as *in situ* observations) and remote sensing. The former provides an instantaneous picture (specific values), while radiometers onboard satellites measure chl-*a* almost continuously on a synoptic scale based on the ocean color (McClain, 2009). The MODIS (Moderate Resolution Imaging Spectroradiometer) radiometer onboard the Aqua satellite has provided daily images since July 2002, of much of the earth's surface, with a resolution of approximately 1 km^2 (Groom et al., 2019).

The ocean's color can be altered by dissolved and suspended material and bottom characteristics, so the satellite chl-*a* data must be compared with *in situ* observations carried out simultaneously (Groom et al., 2019). This procedure requires a systematic and long-term monitoring program, something challenging to carry out in developing countries where limitations exist for sampling and processing data. In this context, the objective of this study is to describe the seasonal pattern of chl-*a* abundance and distribution in Bahia Magdalena (México) with ready-to-use MODIS-Aqua satellite data from July 2002 to December 2013, from the National Commission for the Knowledge and Use of Biodiversity (CONABIO in Spanish) public database. The first step was to determine the criteria to select MODIS-Aqua data to discard outliers; after that, compare chl-*a* MODIS Aqua data with *in situ* observations carried out from 2002 to 2011; subsequently, *in situ* SP-PBavg and
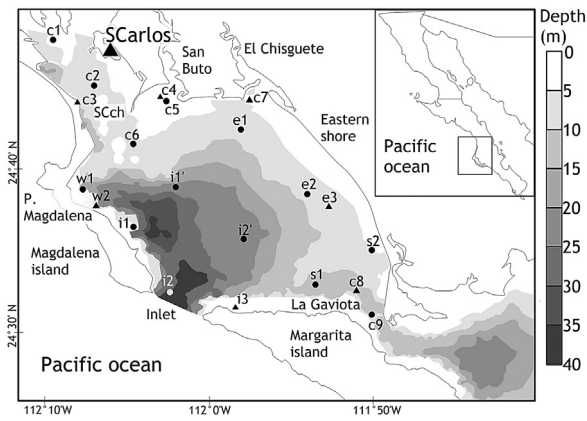
Figure 1 Location of the sampling sites *in situ* (circles) and MODIS-Aqua satellite imagery (circles and triangles). Place names: San Carlos channel (SCch): c1, c2; Pueblo Magdalena: w1, w2; San Carlos channel mouth (SCch mouth): c6; San Buto channel: c5, c4; inlet (Magdalena island): i1, i1′; El Chisguete channel (ECh): e1, c7; lagoon inlet: i2, i2′; the northeastern shore of Margarita island: i3; eastern-central zone: e2, e3; south zone: s1, s2; La Gaviota channel: c8, c9.

distribution pattern were described and contrasted with the MODIS Aqua data patterns.

2. Material and methods

Bahia Magdalena (24.26—25.75°N, 111.33—112.30°W) is in the transition zone between tropical and subtropical environments and is influenced alternately by the California Current (winter—spring) and the Mexican current (summer—autumn) incoming from the Mexican Tropical Pacific and the Gulf of California (Durazo, 2015; Gómez-Valdivia et al., 2015). Global-scale climate phenomena such as the ENSO and the Pacific Decadal Oscillation (Sydeman et al., 2014) alter the regional climate depending on their phase.

Bahia Magdalena is part of the Bahia Magdalena-Bahia Almejas (BM-BA) lagoon system; both lagoons are intercommunicated through the La Gaviota channel (Figure 1). Bahia Magdalena is connected with the ocean by an inlet almost 6 km wide and 40 m deep, located between the Magdalena and Margarita islands (Funes-Rodríguez et al., 2007). The circulation is an anti-estuarine type because in the north and northwest exist shallow channels bordered by mangroves (Figure 1), where evaporation is intense. Nutrient input depends on wind-driven upwelling as well as the state of the tide (Zaytsev et al., 2003).

The type of climate in the region is semi-arid; in San Carlos, a fishing village located north of the lagoon (Figure 1), the average ambient temperature and total annual precipitation are 20.5°C, 98.5 mm, respectively (Ruiz-Corral et al., 2006). The heaviest rains occurred between December and January and also in August and September, associated with the hurricanes' passage.

2.1. Sampling campaigns and gathering of MODIS-Aqua data

Fifty-one sampling campaigns were carried out, lasting one or two days, from April 2000 to December 2011. The sam-

pling frequency was seasonal or semi-annual before 2005, and after that year, it was bimonthly (Table 1). The total number of campaigns per month ranged from 0 (September) to 7 (February). Samples were collected on the surface in 14 sites (marked with a triangle in Figure 1) located at a distance greater than 1.1 km from the coast. Samples for chl-*a* analysis were filtered through GF/F fiberglass filters; the filter's content was used to extract the chl-*a* according to the procedure of Venrick and Hayward (1984). The concentration was estimated with the Jeffrey and Humphrey (1975) method, using a Spectronic Genesys-2 spectrophotometer.

The daily MODIS-Aqua satellite images were processed by the Satellite System for Oceanic Monitoring of the CONABIO (Cerdeira-Estrada et al., 2018), with the methods of Cerdeira-Estrada and López-Saldaña (2011), based on reflectance measured in the channels centered at wavelengths 443, 488, and 551 nm, and incorporated into the OC3M algorithm.

The chl-*a* concentrations of the pixels corresponding to the 14 sites were obtained from daily images from 2011 to 2013, using the wam_pixel_extract tool from WimSoft (https://www.wimsoft.com/mati/). This tool extracted a 3×3 matrix, and its average is assigned to the site. This procedure discarded invalid and outliers. In the chl-*a* distribution analysis, seven other sites were used to expand the sample size (marked with a circle in Figure 1), as described later.

A scatter plot was used to find a correlation between *in situ* and MODIS Aqua data from the same date (Supplementary Figures 1—3). To discard satellite data outliers, we determine an acceptance interval from the shape of the difference between the *in situ* and MODIS Aqua data ($\triangle$chl-$a_{\text{is-sat}}$) distribution and its descriptive parameters (mean, percentiles and kurtosis).

On the other hand, the strategy used to expand the MODIS Aqua sample size used in the comparison with *in situ* data consisted of incorporating data from the days before and after the *in situ* sampling date (chl-a_t). We selected 22 dates with data from one and two days before and after it. Afterward, we compared chl-*a* values (chl-a_t, chl-$a_{t\pm1}$, chl-$a_{t\pm2}$, chl-$a_{\text{prom}-1+1}$) with the non-parametric Kruskal Wallis test (KW-H) and *post-hoc* comparisons methods based on the ranks of the medians of all pairs of groups ($p < 0.05$). All statistical methods were done with Statistica v.8 software (StatSoft, 2007). Finally, we determined the chl-*a* difference between the concentrations ($\triangle$dc$_{\text{sat22}}$=chl-a_{t+n}-chl-a_t) to establish an acceptance interval. These differences ($\triangle$dc$_{\text{sat}}$) were subsequently analyzed in a larger sample (17,555 data pairs) to find a criterion to eliminate outliers.

2.2. Comparison of *in situ* and MODIS Aqua data and SP-PBavg estimation

The differences between *in situ* and MODIS Aqua data (September 2002—December 2011) of 14 sampling sites were assessed from the magnitude of their variance (S). Also, data were compared with the KW-H test and correlated with Pearson's simple correlation analysis applied to transformed data (log n + 1); we use data from the same

Table 1 Sample size in days of the chlorophyll-*a* observations taken *in situ* (in parentheses) and with the MODIS-Aqua satellite. * Days with MODIS and *in situ* data; ** Days with MODIS data one day before or after the *in situ* sampling date. ⁰ Days with *in situ* observations but without MODIS data. TC: total campaigns; note that some campaigns lasted two days.

Year	Jan	Feb	Mar	Apr	May	Jun	Jul	Aug	Sep	Oct	Nov	Dec	Days	TC
2000				(1)								(1)	(1)	1
2001		(1)									(1)		(2)	2
2002					(1)		13 (2)⁰	11	16	25 (1)**	20	18	103 (4)	3
2003	21 (2)**	13 (2)*	14	9	12	16	15	12	16	18	20	17	183 (4)	2
2004	21	17	18	14	14	14	12	14	16	17	16	17	190	
2005	19 (2)*	14 (2)*	20 (1)*	12 (1)⁰	14	14 (1)**	14	14 (1)*	18	19	24 (1)*	20	202 (9)	7
2006	17	23 (1)*	16 (2)*	13 (1)**	14	13 (1)*	12	13 (1)*	13	19 (1)**	20	19 (1)**	192 (8)	7
2007	15	18 (1)*	13	13 (1)**	14	15 (1)**	14	10 (1)⁰	16	24 (1)*	16	20 (1)**	188 (6)	6
2008	17	18 (1)⁰	22	13 (1)*	13	14 (1)*	14	13 (1)**	18	21 (2)*	16	15 (1)**	194 (7)	6
2009	16 (1)**	18 (1)*	10	12 (1)*	11	13 (1)**	14	15 (2)**	14	20 (2)*	23	22 (2)**	188 (10)	7
2010	23	15	20 (1)**	13 (2)**	15	15 (2)**	13	15 (1)**	18	24 (2)**	25	22 (2)**	218 (10)	6
2011	22	21	18	16	11 (1)⁰	13	23	20 (1)*	25	28 (1)*	25	21 (1)**	243 (4)	4
2012	20	25	25	24	24	22	22	21	18	27	19	14	261	
2013	23	19	26	24	23	22	16	23	27	24	5	24	256	
Days	214 (5)	201 (9)	202 (4)	163 (8)	165 (2)	171 (7)	182 (2)	181 (8)	215	266 (10)	229 (2)	229 (8)	2418 (65)	
TC	4	7	3	6	2	6	1	7		7	2	6		51

date (n=450) and one day before or after the *in situ* samplings (n=646), referred as expanded database. There was no MODIS Aqua data from the May and July surveys due to the significant cloud cover.

Chl-*a* concentrations of each data set were grouped by month to calculate the SP-PBavg of all sampling sites and by each site. The KW-H test and *post-hoc* comparison methods were applied to raw *in situ* observations and transformed (log n + 1) MODIS Aqua data to identify the significantly different periods assuming that monthly concentrations were independent of each other.

The *in situ* chl-*a* distribution was described by a hierarchical cluster analysis (CA) carried out by the Unweighted Pair Group Average method using arithmetic averages and a non-metric three-axis Multidimensional Scaling Analysis (MSA). These methods were not used in MODIS Aqua data of the *in situ* samplings dates because of the small sample size, which was insufficient even with the expanded database.

2.3. SP-PBavg and distribution of MODIS Aqua data

The MODIS Aqua SP-PBavg and distribution were assessed with the described methods, applied to the transformed data (log n + 1) from 21 sites (Figure 1) spanned from July 2002 to December 2013. In the first case, all the available data were used (n = 41,525), while in the distribution assessment, only those from the same date were utilized to maintain the same sample size per site (n per site = 774). In addition to the CA and MSA, a Principal Component Analysis (PCA) was applied under the assumption that each PC represents an area of the lagoon. The normalized Varimax rotation was performed to obtain a clear pattern of loadings. Factor scores of each PC were used to describe the SP-PBavg, and the average of the site's data with higher factor loadings was used to estimate the average of each month.

3. Results

3.1. Criteria for selecting satellite information to compare with *in situ* data

The $\triangle$chl-$a_{is\text{-}sat}$ frequency distribution was left-skewed (−2.24) and the mean ± 95% confidence interval (avg ± ci_{95}) was negative (−5.09 ± 0.97 mg m^{-3}; n = 225), indicating that MODIS Aqua overestimated chl-*a* concentration. The shape of the data distribution was very acute (kurtosis: 6.36), so extreme differences (−45.04 and +5.24 mg m^{-3}) could be considered outliers. The interval used for selecting MODIS Aqua data was limited by −6.56 mg m^{-3} (percentile 0.25) and 3.52 mg m^{-3} (percentile 0.99).

In comparing the MODIS Aqua data of consecutive days, only the avg chl-$a_{t\pm1}$ was significantly different (p <0.05), so they were discarded. The $\triangle$dc$_{sat22}$ avg ± ci_{95} between the sampling date and the days before and after was −0.92 ± 0.66 mg m^{-3} (n = 506). The percentiles of 0.25 (−1.78 mg m^{-3}) and 0.75 (0.78 mg m^{-3}), and the kurtosis (9.25), indicated that the difference between consecutive days was small.

The $\triangle$dc$_{sat}$ avg ± ic$_{95}$ was −0.53 ± 0.12 mg m^{-3} and there was no difference between the sites (H (20,

N = 17,555) = 26.96 p = 0.13). Differences among the months were significant (H>20, p <0.05) in the center (i2′) and the eastern shore (c7, e2, and e3), but the *post-hoc* tests were not significant, although the graphs showed great variations between May and July. Based on these results, MODIS Aqua data from one day before or after the date sampling were used. On the other hand, since the $\triangle$dc$_{sat}$ was lower than the $\triangle$chl-$a_{is\text{-}sat}$, data to expand the sample were selected with the same criteria as the satellite data of *in situ* observations dates (−6.56 to 3.52 mg m^{-3}).

3.2. Comparison between *in situ* and MODIS Aqua data

The mean (± confidence interval$_{95}$) $\triangle$chl-$a_{is\text{-}sat}$ was 5.09 ± 0.97 mg m^{-3} (n = 225); it was lower near the lagoon inlet ($\approx$ −1 mg m^{-3}) than to the channels (<−10 mg m^{-3}). The variance (S) of the *in situ* and MODIS Aqua chl-*a* data differences (Table 2A) was smaller (S<10.65) near the inlet (i2, i2′) and Magdalena island (i1 and w1). In contrast, the highest S values (S>80) occurred in the San Carlos channel (c1, c2) and the mouths of the San Buto (c5) and the El Chisguete (e1) channels.

In the San Carlos channel, its mouth (c6), and along the eastern shore (e1, e2, s2) of the lagoon, the chl-*a* measured by the two methods was significantly different according to with KW-H test (Table 2 B) using satellite data of the same date of sampling or the expanded sample. In contrast, there were no significant differences near Magdalena island (w1, i1, i1′) nor the lagoon inlet (i2, i2′).

Scatter plots showed a significant correlation between *in situ* and MODIS Aqua (Supplementary Figures 1—3); however, the correlation coefficient (R=0.32) was low due to satellite data dispersion, especially in the channels (Supplementary Figure 1). The highest correlation coefficients were from the western coast, from Pueblo Magdalena (w1) to the inlet's vicinity (i1, i1′, i2′), as is shown in figures 2 and 3 of Supplementary data. After applying the criteria established in the 3.1 section, Rs increased significantly in almost all sites (Table 2B), except in the San Carlos channel interior (c1) and La Gaviota (c9), where correlation coefficients were close to zero due to small sample size when using the data selection criteria.

3.3. Seasonal pattern and distribution of chl-*a* according to *in situ* data

The SP-PBavg calculated with all *in situ* data (Figure 2A) showed significant differences between the months (KW-H (8, 566) = 124.84; p<0.01). The highest concentrations occurred in June, August, and October, while the lowest in January (p<0.05). This pattern was observed in the northern section of the San Carlos channel (c1), the inlet (i2, i2′), and its surroundings (i1, i1′), the southwestern area (s1), and the La Gaviota channel. In contrast, there were no significant differences (p>0.05) in the rest of the sites, where, although there was a peak of abundance in June or August, it was not significant because of the dispersion of data recorded in other months (March and October, mainly).

Dendogram shows that the lagoon can be separated into two large areas (Figure 2B). One of them includes the

Table 2 Comparison of *in situ* and satellite data. A) Variance of the differences (S). B) Results of the non-parametric Kruskal-Wallis test (KW-H) applied to the raw data and of the Pearson's (R) correlation analysis to the transformed ones (log n + 1), from the same date and immediately before or after that (expanded sample). * p<0.05, D.F degrees of freedom.

A)

Site	Data number	Mean difference (mg m^{-3})	Standard deviation (mg m^{-3})	Variance (S)
c1 San Carlos	70	−14.66	11.5	130.35
c2 San Carlos	84	−9.9	9.4	87.38
c5 San Buto	61	−13.29	9.61	90.76
c6 San Carlos mouth	89	−2.65	4.45	19.58
c9 La Gaviota	63	−6.14	6.46	41.09
e1 El Chisguete-ES	58	−6.5	9.87	95.74
e2 ES	61	−5.56	6.22	83.62
w1 Pmagdalena	63	−1.15	3.29	10.65
i1 MI-WS	60	−0.61	2.03	4.06
i1′ MI-WS	84	−1.12	4.4	19.16
i2 Inlet	78	−0.21	2.28	5.15
i2′ Center-inlet	85	−1.23	2.68	7.13
s1 SW	85	−3.15	4.36	18.75
s2 SE	53	−8.17	6.91	46.87
Total	994	−5.06	5.81	44.86

B)

	KW-H same date	DF	R	KW-H expanded sample	DF	R
All data	**93.73***	**1, 454**	**0.47***	**74.91***	**1, 634**	**0.58***
c1 San Carlos	22.91*	1, 32	0.15	4.86*	1, 16	-0.09
c2 San Carlos	20.46*	1, 36	0.15	15.88*	1, 38	0.68*
c5 San Buto	16.20*	1, 26	0.37	5.33*	1, 8	0.99*
c6 San Carlos mouth	9.01*	1, 40	0.42*	11.96*	1, 68	0.44*
c9 La Gaviota	12.34*	1, 22	0.63*	11.00*	1, 22	0.03
e1 El Chisguete-	10.94*	1, 26	0.69*	14.41*	1, 36	0.48*
e2 East	13.17*	1, 30	0.43	20.84*	1, 42	0.48*
w1 PMagdalena	2.04	1, 30	0.17	0.4	1, 48	0.79*
i1 MI-WS	0.818	1, 36	0.72*	0.79	1, 54	0.77*
i1′ MI-WS	2.027	1, 36	0.84*	2.02	1, 68	0.73*
i2 Inlet	0.17	1, 38	0.35	1.06	1, 64	0.63*
i2′ Center-inlet	2	1, 38	0.37	2.89	1, 74	0.45*
s1 SW	9.61*	1, 36	0.56*	18.21*	1, 68	0.52*
s2 SE	17.86*	1, 28	0.1	14.89*	1, 28	0.54*

sites near the channels: San Carlos and its mouth in Bahía Magdalena, the La Gaviota, and the San Buto's mouth. The rest of the water body is in another area, except for Pueblo Magdalena, which separates from the two clusters. The dendrogram also shows differences between the inlet of the lagoon (i2, i2′, i1′, i1) and the eastern (e1, e2) and southern zones (s1, s2).

The MSA highlights the separation between the channels' mouth and the water body. In Dimension 1, associated with chl-*a* abundance, the sites with the minimum (lagoon inlet) and maximum concentrations (San Carlos channel) are in the opposite positions (Figure 2C). Dimension 2 shows the separation of the western (positive segment) and eastern coast (negative segment) and also that chl-*a* concentrations near the inlet, the center of the lagoon, and the southeastern zone are closer among them than of the northern sites (see circles in Figure 2C). Dimension 3 (not shown in this document) remarks differences between the sites near the La Gaviota and the San Carlos channels.

According to their proximity in the MSA graph (Figure 2C), the sites were grouped into three sets to estimate the SP-PBavg. The three showed significant differences between the months (KW-H>40; p<0.05), although some overlapped in the *post-hoc* tests, probably due to the small sample size. The mean chl-*a* concentration ± standard deviation (avg ± st. dev.) was 2.14 ± 1.79 mg m^{-3} near the inlet (Set 1; Figure 2E), and the higher abundances occurred in March, April and, June (Table 3); while, sometimes there were peaks in August and October. The chl-*a* seasonal patterns in front of Pueblo Magdalena (Figure 2D) and the center of the eastern shore (e2; Figure 2F) peak in June and April, and they were similar to that of the inlet.

The chl-*a* concentration was intermediate in the south (s1, s2) and in front of the El Chisguete channel (Set 2; Figure 2I), there were peaks in March, June, August, and October; in contrast with Set 1, the chl-*a* abundance in April was highly variable. In the third set, formed by the sites located in the San Carlos channel, the La Gaviota chan-
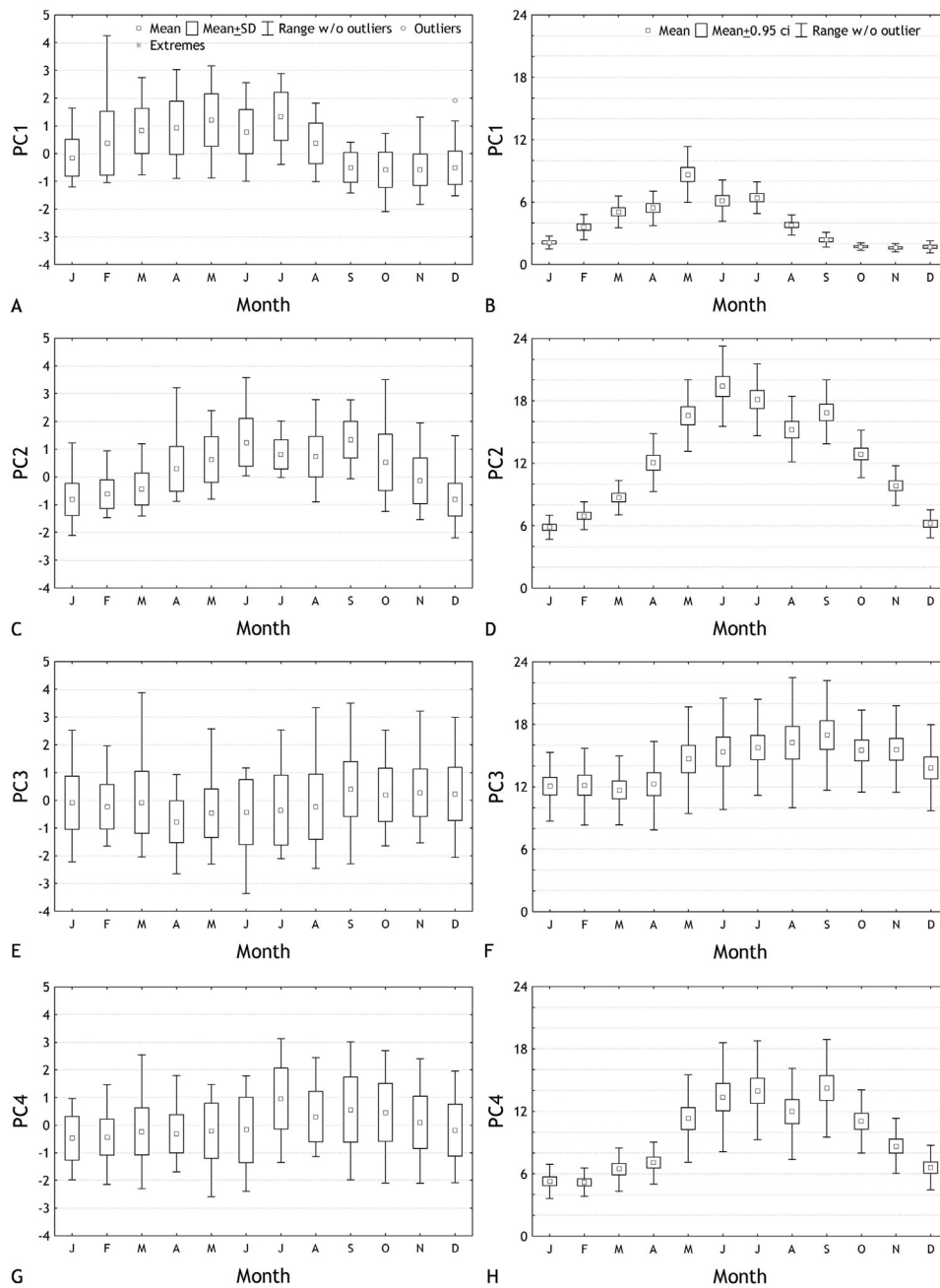
Figure 2 Seasonal patterns from *in situ* observations (A). Dendrogram of cluster analysis (B) and a scatterplot of MDA (C). Panels D—I show the seasonal patterns according to the MDA results and are organized in the same way. The location of the sites is shown in Figure 1.

nel, and in front of the San Buto channel, the highest chl-*a* concentrations occurred from June to October (Figure 2H), with peaks in June, August, and October (Table 3). The highest average levels were found in this area, and there were specific values higher than 12 mg m^{-3}. On the other hand, concentrations at the San Carlos channel's mouth (c6; Figure 2G) were intermediate between Set 3 and Pueblo Magdalena.

3.4. Seasonal pattern calculated with the same dates *in situ* and remote sensing observations

The SP-PBavg calculated with all the *in situ* and satellite data were correlated (r = 0.57; p<0.01), with higher chl-*a* concentrations between March and October and a peak in June (Figure 2A and 3A) when *in situ* specific observations

Table 3 Average (Avg.) concentration and standard deviation (St. dev.) of the three sets of sites identified with the MSA. Set 1 (i1, i1', i2, i2'), Set 2 (s1, e1, s2), Set 3 (c9, c2, c1, c5). Units [mg chl-a m^{-3}].

Months	Set 1			Set 2			Set 3		
	N	Avg.	St. dev.	N	Avg.	St. dev.	N	Avg.	St. dev.
Jan.	12	0.64	0.21	9	0.86	0.28	11	1.54	0.81
Feb.	28	1.64	1.26	21	1.20	0.68	28	2.13	0.98
Mar.	11	2.44	1.44	9	3.47	2.19	11	2.40	1.20
April.	19	2.43	1.58	13	2.31	2.04	18	2.56	1.10
June	21	4.67	1.84	17	3.86	2.64	21	5.09	3.95
Aug.	26	1.78	1.08	19	3.49	1.10	25	5.46	3.23
Oct.	22	1.82	1.63	18	3.33	2.22	24	3.88	1.79
Dec.	21	1.52	1.77	16	1.92	1.43	22	2.34	1.14
Total avg.	160	2.14	1.79	122	2.59	1.99	160	3.36	2.55

Table 4 Factor loadings from the unrotated and rotated Principal Component (PC) Analysis.

Site	Unrotate				Rotate			
	PC 1	PC 2	PC 3	PC 4	PC 1	PC 2	PC 3	PC 4
c4	−0.66	−0.51	−0.01	0.30	0.06	**0.76**	0.42	0.13
c7	**−0.73**	−0.40	0.13	0.24	0.16	**0.80**	0.26	0.20
e3	**−0.80**	−0.24	0.36	0.14	0.29	**0.82**	0.00	0.29
c8	−0.62	**−0.53**	0.14	−0.39	0.05	0.47	0.23	**0.74**
i3	**−0.74**	0.34	0.07	−0.29	**0.75**	0.20	−0.05	0.39
w2	**−0.74**	0.49	−0.21	0.07	**0.88**	0.19	0.16	−0.03
e9	**−0.73**	−0.21	−0.20	0.12	0.37	0.52	0.45	0.16
c1	−0.19	**−0.59**	**−0.62**	−0.01	−0.18	0.09	**0.84**	0.16
c2	−0.59	−0.45	**−0.49**	0.00	0.16	0.34	**0.76**	0.25
w1	**−0.75**	0.42	−0.25	0.03	**0.85**	0.19	0.22	0.02
c6	**−0.77**	0.05	−0.27	−0.05	0.60	0.31	0.39	0.23
c5	**−0.72**	−0.51	−0.05	0.24	0.11	**0.76**	0.46	0.20
i1	−0.68	**0.62**	−0.13	0.03	**0.92**	0.11	0.01	−0.05
i1'	**−0.70**	**0.60**	−0.08	−0.05	**0.92**	0.11	−0.03	0.05
e1	**−0.83**	0.08	0.16	0.16	0.58	0.63	0.04	0.13
i2	−0.69	**0.56**	−0.01	−0.06	**0.87**	0.15	−0.07	0.07
i2'	−0.70	**0.58**	0.06	−0.07	**0.88**	0.18	−0.14	0.09
e2	**−0.81**	0.01	0.33	0.22	0.48	**0.75**	−0.07	0.13
s1	**−0.75**	−0.20	0.14	**−0.44**	0.37	0.39	0.12	**0.72**
s2	−0.69	−0.41	0.31	0.05	0.12	**0.76**	0.08	0.38
c9	−0.40	**−0.50**	0.02	**−0.54**	−0.05	0.20	0.26	**0.77**
Explained variance	10.14	4.01	1.31	1.05	6.70	5.11	2.34	2.36
%	0.48	0.19	0.06	0.05	0.32	0.24	0.11	0.11

were higher than 5 mg m^{-3}; however, the MODIS Aqua data exceed them several times.

3.5. SP-PBavg and identification of areas in the lagoon with MODIS Aqua data

The SPs calculated with the satellite data of the 21 sites (Figure 3B) were well-defined (p<0.05), even near the channels, where the *in situ* observations were highly variable. In general, chl-a concentrations were higher in spring and early summer, with another small peak in September, in early fall (Figure 3B). The 0.75 percentile showed that most of the data was less than 18 mg m^{-3}; however, some reached 60 mg m^{-3} in all months.

CA showed the lagoon could be divided into two large areas according to the chl-a concentration, like *in situ* observations (Figure 3C). The first was composed of sites located at the mouth of the San Buto and the El Chisguete channels, the San Carlos channel, and La Gaviota and its surroundings (c8, s2). The second has two sub-zones: the first covers from Pueblo Magdalena to the northwestern part of Margarita island (i3), including the inlet and surrounding area. On the
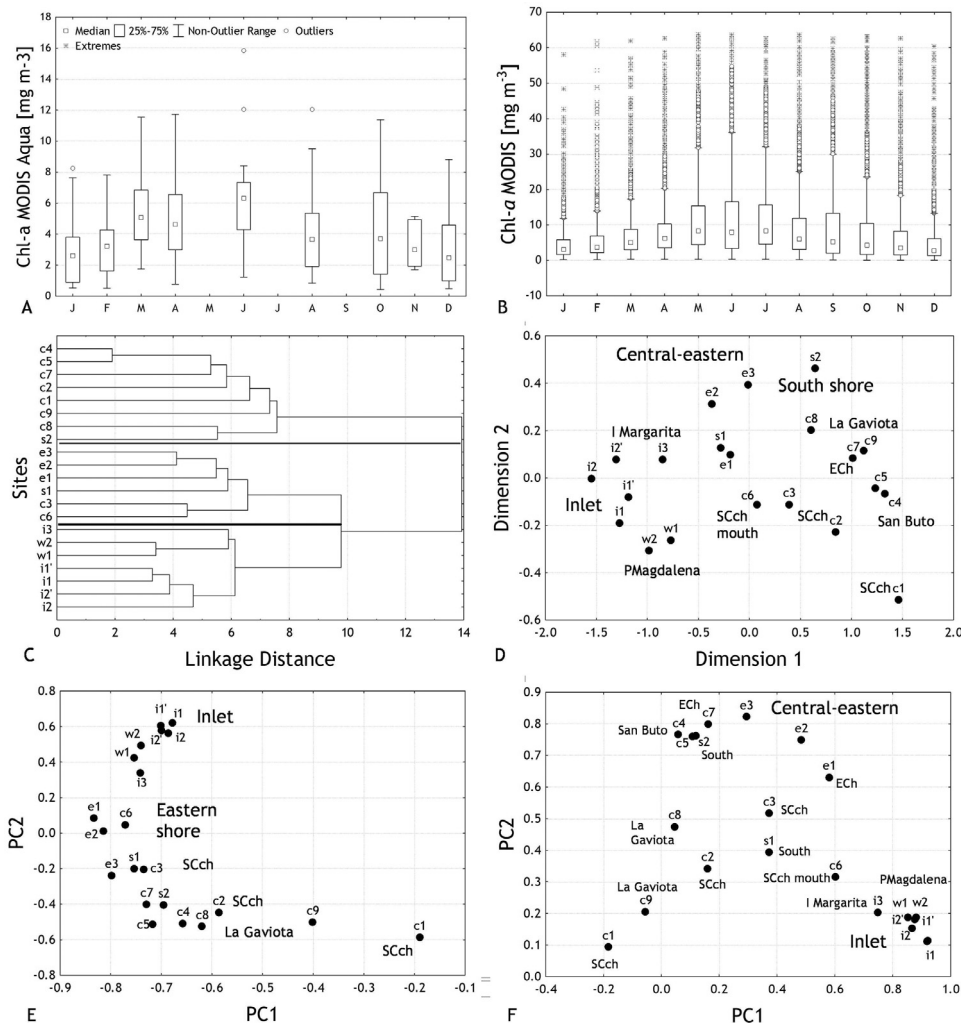
Figure 3   Seasonal patterns obtained with data from the MODIS-Aqua satellite, from the same dates of the *in situ* samplings (A) and all data (B). Results of the application of multivariate statistical methods. Dendogram of cluster analysis (B), here black lines show conglomerates; diagram of the non-metric MSA applied to the transformed MODIS data (n_{month} = 774). Ordination plots resulting from unrotated (E) and rotated (F) PCA.

other are the eastern shore (e3, e2, c7, s1) and the San Carlos channel's mouth (c3, c6).

The sites' arrangement in the MSA diagram (Figure 3D) was equivalent to that of the *in situ* observations. We analyzed transformed data (log n + 1) to diminish the localities' distance due to magnitude differences in chl-*a* concentrations. In dimension 1, associated with concentration, in the extreme left are sites near the lagoon inlet and on the right the places near the La Gaviota and the San Buto channels, while the rest are in the middle part. The sites located in the inlet, the center, and the south-southeast zone are in the positive segment of dimension 2, but the extreme values are from the east (e3, e2) and southeast shores (s2). On the negative segment are the lagoon's northern and western zones, between the inlet and Pueblo Magdalena, although the smallest value is in the north part of the San Carlos channel (c1). In dimension 3 (not shown), the highest values correspond to the La Gaviota channel, while the lowest to the sites near the El Chisguete channel.

The first four components of the unrotated PCA accounted for 78% of the explained variance. PC1 explained

48%, and most of the sites significantly correlated with it (>|0.7|), except for the channels' mouth and the inlet (Table 4). The PC2 explained 19% of the variance, and the highest factor loadings were from the lagoon inlet (with positive values), the channels (with negative values), and the La Gaviota channel (Figure 3E). The PC3 and PC4 explained around 5% each one, and sites in the San Carlos and the La Gaviota channels had the highest factor loadings in each component.

The explained variance of the first four components in the rotated PCA was more homogeneous and diminished the number of sites correlated significantly with each PC (Figure 3F, Table 4). On the other hand, the factor scores of the four PCs showed well-defined SP-PB (KW-H (11,774)>85, p<0.01). The PC1 accounted for ≈31% of the variance. The sites with the highest factor loadings (Figure 3F) were on the western shore, from Pueblo Magdalena (w2) to the northwestern of Margarita island (i3), including the lagoon inlet (i1, i1′, i2, i2′). In this area, chl-*a* concentration was high from March/April to July and scarce from September to December—January (Figure 4A), while there were wide
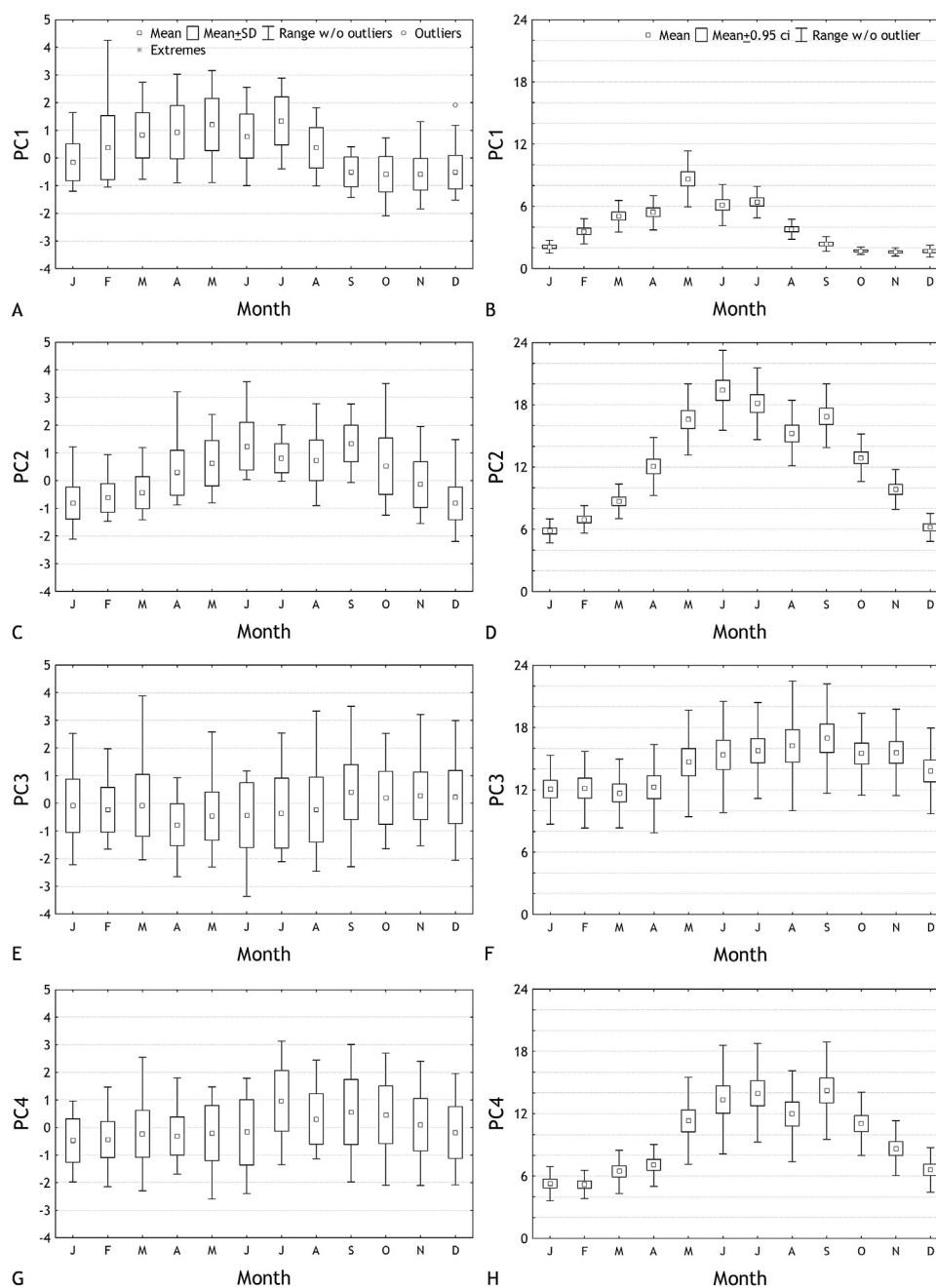
Figure 4 Seasonal chl-*a* patterns described by the factor scores of the four principal components (PC) resulting from the PCA (left column) and the mean values of the sites (± confidence interval) with the highest factor loadings in each PC (right column; units: mg m^{-3}). In the left column graphs, the boxes represent the mean ± the first standard deviation, and the whiskers two standard deviations; in the right, the mean±95% confidence interval, and the whiskers range without outliers.

variations in February. The general avg ± ci$_{95}$ was 3.75 ± 0.09 mg m^{-3}, and the maximum concentrations were observed from May (8.66 ± 0.67 mg m^{-3}) to July (6.44 ± 0.39 mg m^{-3}), with a slight decrease in June (Figure 4B, Table 5).

The highest factor loadings in the PC2 (24% of explained variance) corresponded to the eastern shore sites (c4, c7, e3, c5, e2, and s2; Figure 3F), with a general average of 11.75 ± 0.19 mg m^{-3}. Chl-*a* concentrations of the sites included in this PC and subsequent were significantly different from *in situ*. In the PC2 sites, correlations between

in situ and MODIS Aqua were significant, suggesting that the satellite detected other elements, including the organic matter contribution from other plants and sources, and we use the term chl-*a*+om (other materials). Chl-*a* +om was high for a more extended period than in the western shore, spanning from April/May to October with peaks in June (19.39 ± 0.96 mg m^{-3}) and September (16.89 ± 0.79 mg m^{-3}); although there may be large concentrations in October (Figure 4C and D). The lowest concentrations occurred from December to March, and in November and April were intermediate (Figure 4D).

Table 5 Descriptive statistical parameters (avg, ci$_{95}$) of the four principal components (PC). Units: [mg chl-a m^{-3}].

	PC1			PC2			PC3			PC4		
Month	Avg	Ci$_{95}$	N	Avg	Ci$_{95}$	N	Avg	Ci$_{95}$	N	Avg	Ci$_{95}$	N
Jan.	2.12	0.15	1,154	5.85	0.29	970	12.07	0.84	313	5.28	0.41	435
Feb.	3.61	0.30	1,177	6.96	0.34	950	12.16	0.96	293	5.18	0.34	454
Mar.	5.06	0.38	1,142	8.71	0.42	912	11.70	0.85	296	6.46	0.54	426
Apr.	5.43	0.42	892	**12.06**	0.70	655	12.25	1.11	220	7.08	0.52	306
May	**8.66**	0.67	940	**16.58**	0.87	684	**14.67**	1.32	243	**11.31**	1.06	309
June	**6.14**	0.50	963	**19.39**	0.96	709	**15.39**	1.40	230	**13.37**	1.33	321
Jul.	**6.44**	0.39	985	**18.13**	0.87	701	**15.78**	1.16	250	**13.97**	1.21	330
Aug.	3.81	0.25	971	**15.24**	0.81	673	**16.24**	1.57	231	**11.98**	1.16	307
Sept.	2.38	0.18	1,140	**16.89**	0.79	810	**16.96**	1.37	259	**14.25**	1.20	365
Oct.	1.73	0.09	1,608	**12.90**	0.57	1,262	**15.49**	1.01	380	**11.05**	0.77	596
Nov.	1.61	0.10	1,429	9.86	0.48	1,148	**15.61**	1.04	371	8.66	0.67	528
Dec.	1.70	0.15	1,280	6.20	0.34	1,100	13.82	1.05	339	6.60	0.55	509
Total	3.75	0.09	13,681	11.75	0.19	10,574	14.32	0.33	3,425	9.28	0.25	4,886

In PC3 and PC4 (Figure 4E—H), which explained 11% of the variance each, the most important sites were in the San Carlos channel (PC3: c1, c2) and the southern zone near La Gaviota (PC4: s1, c8, and c9). Chl-a+om was abundant throughout the year in the San Carlos channel ($>$10 mg m^{-3}), and the annual average coefficient of variation was 0.22, the smallest of the four PC. On the other hand, although the PC3 factor scores (Figure 4E and F) showed significant differences (KW-H (11, 774) = 85.174; p $<$0.01), the results of the *post-hoc* test were not conclusive, although suggested that there were differences between the periods May—November and December—April (Table 5). The graph of PC4 showed that the period in which chl-a+om was higher is out of phase with PC1 and PC2 because it spanned from May/June to October ($\approx$10 mg m^{-3}), while it was scarce from January to April (Figure 4G—H). On the other hand, the PC3 and PC4 seasonal patterns were similar to *in situ* third set.

4. Discussion

This study aims to describe the time and spatial patterns of chl-a with the ready-to-use MODIS-Aqua public database, which uses the OC3M algorithm designed for marine waters with low-content sediments and colored dissolved organic matter. Therefore, this section focused on the use advantages and limitations of this database in Bahia Magdalena and later in the chl-a abundance and distribution patterns.

Climatologies usually represent the average of a recent 30-year period of any variable; however, recent studies concluded that ten years are enough to reflect the average variability (Word Meteorological Organization, 2017). The regular monitoring of the *in situ* chl-a over long periods is very expensive; in comparison, ocean color satellite data ready-to-use has been available in public databases almost continuously since 1997 when the Sea-viewing Wide field-of-view (SeaWifs) radiometer began operations. By 2020, the MODIS-Aqua, NOAA JPSS VIIRS, and ESA Sentinel 3 OLCI sensors were active. However, in this study, only the MODIS-Aqua data are used to obviate the sensors' differences (Groom et al., 2019).

Identifying the chl-a variability of intra and inter-annual scales is a big challenge in studying coastal lagoons (Beer and Joyce, 2013). Bimonthly *in situ* observations carried out from 2005 to 2011 were used to estimate the seasonal variability and its relationship with fertilization mechanisms (Jiménez-Quiroz et al., 2019). Analyses applied to *in situ* observations in this study suggest three zones with different dynamics. In the inlet, chl-a concentration is lower than in the rest of the lagoon, peaking in spring. In contrast, there are two peaks in the eastern and southeastern zones: late winter and late spring to early autumn; while in the vicinity of the channels (San Carlos, La Gaviota) and at the mouth of the San Buto and El Chisguete channels from late spring to early autumn, a more extended period. However, the sampling frequency omitted information from relevant months such as May and July, and on the other hand, the sample size was small ($<$30 observations per month), and the data dispersion high. *In situ* data describes the SP-PBavg coarsely but only outlines the chl-a distribution in the lagoon.

4.1. Advantages and limitations of MODIS Aqua data using in Bahia Magdalena

The MODIS-Aqua imagery used spans for just over ten years (July 2002—December 2013), so the climatology complies with the World Meteorological Organization. We did not use more recent data to avoid the drastic changes caused by anomalous warming due to the 2014—2015 "The Blob" and the 2015—2016 ENSO in the Northeast Pacific and Bahia Magdalena (Jiménez-Quiroz et al., 2019; Leising et al., 2015).

The MODIS Aqua imagery spatial resolution (1 km^2) is appropriate for this lagoon study because it is approximately 68 km long and 45 km wide. Even the San Carlos channel width in its southern part is 10 km, and the inlet is around 6 km. The region's arid characteristics and lack of river discharges diminish the interference of suspended sediments in remote sensing analysis; in the same way, the supply of sediments during tropical storms is limited (Sanchez et al., 2010). Another favorable feature of Bahia Magdalena is that macrophytes (mangroves, seagrass, macroalgae) are abundant only in the shallow channels in the north and south-

east areas (Chávez-Rosales, 2006; Funes-Rodríguez et al., 2007; Hernández-Carmona et al., 2007), and fine-grain sediments (silt and mud) are confined to mangal zones. There are some mangals on the eastern shore of Magdalena island, but they are very sparse. Mangal coverage in Banderitas (29 km^2) and Bahia Magdalena (31 km^2) is small (González-Zamorano et al., 2003), and their organic matter supply is restricted to this relatively small area, compared with the water body (883 km^2).

The main limitation of MODIS-Aqua is related to the water characteristics and the algorithm used to calculate chl-*a* concentration. The channels' vicinity characteristics resemble Case-2 waters, whereas the OC3M algorithm was designed for Case-1 waters (Hu et al., 2012). However, except for the San Carlos (c1) and La Gaviota channels (c9), where the *in situ* and MODIS Aqua data were no correlated (R≈0) due to the small sample size (n<10), Rs were significant in the mouth of the other channels. On the other hand, both c1 and c9 data were significantly correlated with their next neighbors when used all satellite data (n per site = 774). There are processing algorithms that improve chl-*a* detection capabilities in MODIS images (Hu et al., 2012). Also, there are currently new algorithms that allow chlorophyll detection in Case-2 waters developed for the MERIS and OLCI satellite sensors of the European Space Agency. However, its use is beyond this study's scope, focused on the applicability of ready-to-use imagery.

This study's other limitations are related to the techniques used for *in situ* measurements of chl-*a*, based on the spectrophotometric method and the Jeffrey and Humphrey (1975) equations. This method is very used because of is easily done in the laboratory and is reasonably accurate where chl-*a* degradation products are absent (Aminot and Rey, 2000), which could be the case in the inlet, while its precision probably diminishes in the channels' vicinity.

The varying sample size between the months could be a problem because there were more MODIS Aqua images from October to February, probably due to the cloudiness even though rainfall is scarce in the region (Ruiz-Corral et al., 2006). However, since the sample size was large in all months, we assume that the mean is representative.

4.2. Climatology estimated with satellite information

The MODIS Aqua chl-*a* concentrations were statistically similar to the *in situ* observations near the lagoon inlet, suggesting that its characteristics are similar to the marine ones, classified as Case-1 water, where the chl-*a* concentration covaries with the rest of the optically active components. On the other hand, the variance explained from PC1 of rotated PCA (31%) indicates that this zone represents a high percentage of the chl-*a* variability in Bahia Magdalena.

In this area, the phytoplankton biomass is more abundant from March/April to July and also is more constant because the dispersion of April, May, and June data is less than that of other months; this period corresponds to spring upwelling season (Jiménez-Quiroz et al., 2019). The opposite occurs from October to December, possibly due to the high variability of environmental phenomena that influence fertilization mechanisms, such as the northwesterly wind, tropi-

cal storms, and hurricanes, but that should be addressed in future studies.

The chl-*a* concentration measured with the two methods on the eastern shore, where the sampled sites' water depth is greater than 10 meters, was significantly different. However, its variability was similar and showed higher concentrations during a more extended period than in the inlet (April/May to October). This pattern coincided with *in situ*, suggesting that MODIS Aqua detected the chl-*a* signal, but other elements interfere with the measurements. The explained variance pf PC1 and PC2(≈32 and 24%, respectively) suggest that MODIS Aqua data describe almost half of chl-a variability in Bahia Magdalena, suggesting that it is a useful tool in future studies.

In the channels' surroundings (San Carlos, San Buto, El Chisguete), high concentrations occur almost all year. We assumed that satellite measures chl-*a,* and other materials, including phaeophytin-*a*, other degradation substances, and colored organic matter supplied by other vegetables. Macroalgae and seagrass mortality occur at the end of spring when the temperature increases (Hernández-Carmona et al., 2007; Santamaría-Gallegos et al., 2007) while mangrove defoliation in summer-autumn is high due to high temperatures and the passage of hurricanes (Chávez-Rosales, 2006). Additionally, in autumn, there may be algal blooms triggered by the re-suspension of nutrients from the sediment caused by the vertical mixing in the water column forced by the northwesterly winds (Jiménez-Quiroz et al., 2019; Gárate-Lizárraga and Siqueiros-Beltrones, 1998). *In situ* chl-*a* data also were high, but they did not show a seasonal trend due to the small sample size.

This pattern suggests another production period in the lagoon's interior, independent of the nutrients' upwelling supply, associated with the detritus food chain, which could explain the high productivity of Bahia Magdalena all year round.

An indicator of the lagoon's food availability is the continuous reproduction of several bivalves and their average oocyte size. These organisms are filtering-feed, and their phenology coincides with phytoplankton and particulate organic matter seasonal patterns. *Atrina maura* and *Argopecten ventricosus* reproduce all year-round, with peaks in winter and spring (Félix-Pico, 2006). *Chione* spp. and *Pinna rugosa*, habits in the channels zone and reproduce mainly in summer—autumn. *Megapitaria squalida*, which lives in channels and their mouth, has reproductive peaks in spring and autumn (Amezcua-Castro, 2014). *M. squalida, A. maura*, and *A. ventricosus* oocytes size are bigger in this lagoon than in La Paz and other Baja California locations (Amezcua-Castro, 2014; Camacho-Mondragón, 2014; Romo-Piñera, 2010), due to its high chl-*a* and organic matter concentrations (Romo-Piñera, 2010).

4.3. Seasonal variations in chlorophyll and cell density

The SP-PB patterns estimated were similar to the variations of phytoplankton cell density in the interior (Jiménez-Quiroz et al., 2019; Garate-Lizárraga and Siqueiros-Beltrones, 1998) and the marine area adjacent to Bahia Magdalena (Martínez-López, 1993) even tough cell density is not equivalent to biomass (Cornet-

Barthaux et al., 2007). Samples carried out discontinuously between 1980 and 1989 (Gárate-Lizárraga I. et al., 2001; Gárate-Lizárraga and Siqueiros-Beltrones, 1998; Martínez-López, 1993; Nienhuis and Caballero, 1985), showed that high cell densities ($>250 \times 10^3$ cells l^{-1}) were more frequent at the end of winter and in spring, and the highest ($>500 \times 10^3$ cells l^{-1}) occurred in March, May, and June, in a similar way to chl-*a* seasonal variability. From 2015 to 2018, high densities ($>500 \times 10^3$ cells l^{-1}) were found from April to July, and they were related to strong upwelling (Jiménez-Quiroz et al., 2019). The sites where the cell density was higher during the spring blooms were the San Carlos channel and its mouth, in front of Pueblo Magdalena, the lagoon's central part, and the eastern shore (1981—1983; 2017, 2019).

Autumn algal blooms were less frequent, and their distribution was widely variable; in the historical record, high cell densities were recorded in November (1982), October (1986), and September (2016), each one with a different extent. Blooms covered almost the entire lagoon, except the inlet and the southwestern in November 1982, and the southwest zone in October 1986 (Gárate-Lizárraga and Siqueiros-Beltrones, 1998). In September 2016, occurred in front of the San Buto channel (Jiménez-Quiroz et al., 2019). MODIS Aqua could improve the detection of these blooms despite the interferences of organic matter and other materials.

5. Conclusions

Our objective was to build a climatology and distribution pattern to use MODIS Aqua's time series in future studies. Chl-*a* concentration measured *in situ* and with the MODIS Aqua satellite was similar (p<0.05) in the inlet and its surroundings (i2, i2′, i1, i1′, w1), indicating that the MODIS Aqua data are a proxy of the chl-*a*. In contrast, on the eastern and southeastern shore (c5, e1, e2, s1, and s2), MODIS overestimated the chl-*a* concentration, but the trend of the two data sets was similar (r>0.5; p<0.05), suggesting that this tool is useful to describe chl-*a* variability. Near the shallow channels (c2, c5, and c6), chl-*a* concentration and data trends were different (r<0.5; p>0.05) due to interference from other factors during the measurements. Since the MODIS Aqua detects the ocean color changes, it probably identifies chl-*a* degradation products, organic matter supplied by mangroves, and other sources, including algal blooms, especially in summer and early autumn.

Acknowledgments

Supplementary materials

Supplementary material associated with this article can be found, in the online version, at https://doi.org/10.1016/j.oceano.2021.03.003.

References

Amezcua-Castro, S., 2014. Uso de áreas de pesca de almeja chocolata (Megapitaria squalida) en Bahía Magdalena-Almejas. Master's thesis. IPN-CICIMAR, La Paz, BCS, México.

Aminot, A., Rey, F., 2000. Standard procedure for the determination of chlorophyll-*a* by spectroscopic methods. International Council for the Exploration of the Sea, Copenhagen.

Beer, N.A., Joyce, C.B., 2013. North Atlantic coastal lagoons: conservation, management and research challenges in the twenty-first century. Hydrobiologia 701, 1—11. https://doi.org/10.1007/s10750-012-1325-4

Behrenfeld, M.J., Boss, E.S., 2014. Resurrecting the ecological underpinnings of ocean plankton blooms. Ann. Rev. Mar. Sci. 6, 167—194. https://doi.org/10.1146/annurev-marine-052913-021325

Bond, N.A., Cronin, M.F., Freeland, H., Mantua, N., 2015. Causes and impacts of the 2014 warm anomaly in the NE Pacific. Geophys. Res. Lett. 42. https://doi.org/10.1002/2015GL063306

Boyer, J.N., Kelble, C.R., Ortner, P.B., Rudnick, D.T., 2009. Phytoplankton bloom status: Chlorophyll *a* biomass as an indicator of water quality condition in the southern estuaries of Florida. USA. Ecol. Indic. 9, S56—S67. https://doi.org/10.1016/j.ecolind.2008.11.013

Camacho-Mondragón, M.A., 2014. Organización de la gónada, gametogénesis, sexualidad y variaciones estacionales y geográficas de las tácticas reproductivas del hacha china *Atrina maura* (Sowerby, 1835) (Bivalvia: Pinnidae). PhD thesis. IPN-CICIMAR, La Paz, BCS, México.

Cerdeira-Estrada, S., López-Saldaña, G., 2011. A novel Satellite-based Ocean Monitoring System for Mexico. Ciencias Marinas 37, 237—247. https://doi.org/10.7773/cm.v37i2.1921

Cerdeira-Estrada, S., Martell-Dubois, R., Valdéz-Chavarin, J., Rosique-de la Cruz, L., Perera-Valderrama, S., López-Perea, J., Caballero-Aragón, H., Ressl, R., 2018. Sistema de Información y Análisis Marino Costero (SIMAR). CONABIO, Cd de Mexico.

Chavez, F.P., Collins, C.A., Huyer, A., Mackas, D.L., 2002. El Niño along the west coast of North America. Prog. Oceanogr. 54, 1—5. https://doi.org/10.1016/S0079-6611(02)00040-X

Chávez-Rosales, S., 2006. El papel de los manglares en la producción de las comunidades acuáticas de Bahía Magdalena. PHD Thesis. IPN-CICIMAR, La Paz, BCS, México.

Cloern, J.E., Foster, S.Q., Kleckner, A.E., 2014. Phytoplankton primary production in the world's estuarine-coastal ecosystems. Biogeosciences 11, 2477—2501. https://doi.org/10.5194/bg-11-2477-2014

Cornet-Barthaux, V., Armand, L., Quéguiner, B., 2007. Biovolume and biomass estimates of key diatoms in the Southern Ocean. Aquat. Microb. Ecol. 48, 295—308. https://doi.org/10.3354/ame048295

Cota-Nieto, J.J., Jiménez-Esquivel, V., Mascareñas-Osorio, I., 2015. La pesca en Bahía Magdalena-Almejas: motor económico para B.C.S. Datamares. https://doi.org/10.13022/M3GW2F

Coupel, P., Matsuoka, A., Ruiz-Pino, D., Gosselin, M., Marie, D., Tremblay, J.-É., Babin, M., 2015. Pigment signatures of phytoplankton communities in the Beaufort Sea. Biogeosciences 12, 991—1006. https://doi.org/10.5194/bg-12-991-2015

de La Lanza-Espino, G., 1994. Fitoplancton y productividad. UABCS, La Paz, BCS.

Durazo, R., 2015. Seasonality of the transitional region of the California Current System off Baja California. J. Geophys. Res. Oceans 120, 1173—1196. https://doi.org/10.1002/2014JC010405

Félix-Pico, E.F., 2006. Mexico, in: Scallops Fisheries and Aquaculture. Elsevier Sci., 1337—1390.

Franco-Gordo, C., Godínez-Domínguez, E., Filonov, A.E., Tereshchenko, I.E., Freire, J., 2004. Plankton biomass and larval fish abundance prior to and during the El Niño period of 1997—1998 along the central Pacific coast of México. Progress in Oceanography 63, 99—123. https://doi.org/10.1016/j.pocean.2004.10.001

Funes-Rodríguez, R., Gómez-Gutierrez, J., Palomares-García, R., 2007. Estudios ecológicos en Bahía Magdalena. CICIMAR-IPN, FONMAR-BCS, La Paz, BCS.

Gárate-Lizárraga, I., Siqueiros-Beltrones, D.A., 1998. Time variation in phytoplankton assemblages in a subtropical lagoon system after the 1982-1983 "El Niño" event (1984 to 1986). Pac. Sci. 52, 79—97.

Gárate-Lizárraga, I., Verdugo Díaz, G., Siqueiros- Beltrones, D.A., 2001. Variations in phytoplankton assemblages during 1988—1989 in a subtropical lagoon system on the west coast of México. Oceánides 16, 1—16.

García-Borbón, J.A., 2019. Variabilidad en la biomasa de camarón café (*Farfantepeanus californiensis*) en Bahía Magdalena — Almejas, Baja California Sur, México. PhD Thesis. Centro de Investigaciones Biológicas del Noroeste, La Paz, BCS.

Geider, R.J., 1987. Light and temperature dependence of the carbon to chlorophyll a ratio in microalgae and cyanobacteria: implications for physiology and growth of phytoplankton. New Phytol 106, 1—34. https://doi.org/10.1111/j.1469-8137.1987.tb04788.x

Gómez-Valdivia, F., Parés-Sierra, A., Flores-Morales, A.L., 2015. The Mexican Coastal Current: A subsurface seasonal bridge that connects the tropical and subtropical Northeastern Pacific. Cont. Shelf Res. 110, 100—107. https://doi.org/10.1016/j.csr.2015.10.010

González-Zamorano, P., Nava-Sánchez, E.H., León de la Luz, J.L., Díaz-Castro, S.C., 2003. Patrones de distribución y determinantes ambientales de los manglares peninsulares. In: E.F., Félix-Pico., Serviere-Zaragoza, E., Riosmena-Rodríguez, R., León de La Luz, J.L. (Eds.), Los Manglares de La Península de Baja California. Centro de Investigaciones Biológicas del Noroeste, La Paz, BCS, 67—102.

Groom, S., Sathyendranath, S., Ban, Y., Bernard, S., Brewin, R., Brotas, V., Brockmann, C., Chauhan, P., Choi, J., Chuprin, A., Ciavatta, S., Cipollini, P., Donlon, C., Franz, B., He, X., Hirata, T., Jackson, T., Kampel, M., Krasemann, H., Lavender, S., Pardo-Martinez, S., Mélin, F., Platt, T., Santoleri, R., Skakala, J., Schaeffer, B., Smith, M., Steinmetz, F., Valente, A., Wang, M., 2019. Satellite Ocean Colour: Current status and future perspective. Front. Mar. Sci. 6. https://doi.org/10.3389/fmars.2019.00485

Hernández-Carmona, G., Serviere-Zaragoza, E., Riosmena-Rodríguez, R., Sánchez-Rodríguez, I., 2007. Flora marina del sistema lagunar de Bahía Magdalena-Bahía Almejas. CICIMAR-IPN, FONMAR-BCS, La Paz, BCS.

Hu, C., Lee, Z., Franz, B., 2012. Chlorophyll a algorithms for oligotrophic oceans: A novel approach based on three-band reflectance difference. J. Geophys. Res. Oceans 117. https://doi.org/10.1029/2011JC007395

Jeffrey, S.W., Humphrey, G.F., 1975. New spectrophotometric equations for determining chlorophylls a, b, c and c2 in higher plants, algae and natural phytoplankton. Biochemie und Physiologie der Pflanzen 167, 191—194. https://doi.org/10.1016/S0015-3796(17)30778-3

Jiménez-Quiroz, M.del C., Cervantes-Duarte, R., Funes-Rodríguez, R., Barón-Campis, S.A., García-Romero, F.de J.,

Hernández-Trujillo, S., Hernández-Becerril, D.U., González-Armas, R., Martell-Dubois, R., Cerdeira-Estrada, S., Fernández-Méndez, J.I., González-Ania, L.V., Vásquez-Ortiz, M., Barrón-Barraza, F.J., 2019. Impact of "The Blob" and "El Niño" in the SW Baja California Peninsula: Plankton and Environmental Variability of Bahia Magdalena. Front. Mar. Sci. 6. https://doi.org/10.3389/fmars.2019.00025

Leising, A., Schroeder, I., Bograd, S., Abell, J., Durazo, R., Gaxiola-Castro, G., Bjorkstedt, E., Field, J., Sakuma, K., Robertson, R., Goericke, R., Peterson, W., Brodeur, R., Barceló, C., Auth, T., Daly, E., Suryan, R., Gladics, A., Warzybok, P.CICESE, 2015. State of the California Current 2014—15: Impacts of the warm-water "Blob". CalCOFI Rep 56, 31—68.

Lynam, C.P., Llope, M., Möllmann, C., Helaouët, P., Bayliss-Brown, G.A., Stenseth, N.C., 2017. Interaction between top-down and bottom-up control in marine food webs. P Ntl. Acad. Sci. USA 114, 1952—1957. https://doi.org/10.1073/pnas.1621037114

Martínez-López, A., 1993. Efectos del evento "El Niño" 1982-1983 en la estructura del fitoplancton en la costa occidental de Baja California Sur. Master's thesis. IPN-CICIMAR, La Paz, BCS.

McClain, C.R., 2009. A decade of satellite ocean color observations. Ann. Rev. Mar. Sci. 1, 19—42. https://doi.org/10.1146/annurev.marine.010908.163650

Nienhuis, H., Caballero, R.G., 1985. A quantitative analysis of the annual phytoplankton cycle of the Magdalena lagoon complex (Mexico). J. Plankton Res. 7, 427—441. https://doi.org/10.1093/plankt/7.4.427

Romo-Piñera, A.K., 2010. Estrategia reproductiva de Megapitaria squalida (Sowerby, 1835) en dos zonas de Baja California Sur. PhD thesis. IPN-CICIMAR, La Paz, BCS, México.

Ruiz-Corral, J.A., Medina-García, G., Meza-Sánchez, R., Díaz Padilla, G., Serrano-Altamirano, V., 2006. Estadísticas climatológicas básicas del estado de Baja California Sur (Período 1961-2003). INIFAP-CIRNO Cd. Obregón.

Sanchez, A., Choumiline, E., Lopez Ortiz, B.E., Aguiniga, S., Sanchez Vargas, L., Romero Guadarrama, A., Rodriguez Meza, D., 2010. Patron de transporte de sedimento en Bahia Magdalena, Baja California Sur, Mexico, inferido del analisis de tendencias granulometricas. Latin American J. Aquat. Res. 38, 167—177. https://doi.org/10.3856/vol38-issue2-fulltext-1

Santamaría-Gallegos, N.A., Félix-Pico, E.F., Sánchez-Lizaso, J.L., Riosmena-Rodríguez, R., 2007. Ecología de la fanerógama Zostera marina en el sistema lagunar Bahía Magdalena-Bahía Almejas. In: Funes-Rodríguez, R., Gómez-Gutiérrez, J., Palomares-García, R. (Eds.), Estudios Ecológicos En Bahía Magdalena. CICIMAR-IPN, FONMAR-BCS, La Paz, BCS, 101—112.

Sommer, U., Stibor, H., Katechakis, A., Sommer, F., Hansen, T., 2002. Pelagic food web configurations at different levels of nutrient richness and their implications for the ratio fish production:primary production. Hydrobiologia 484, 11—20. https://doi.org/10.1023/A:1021340601986

StatSoft, I., 2007. Statistica.

Sydeman, W.J., Thompson, S.A., García-Reyes, M., Kahru, M., Peterson, W.T., Largier, J.L., 2014. Multivariate ocean-climate indicators (MOCI) for the central California Current: Environmental change, 1990—2010. Prog. Oceanogr. 120, 352—369. https://doi.org/10.1016/j.pocean.2013.10.017

Venrick, E.L., Hayward, T., 1984. Determining chlorophyll on the 1984 CALCOFI surveys, XXV. CalCOFI Rep., USA, 74—79.

World Meteorological Organization, 2017. WMO Guidelines on the Calculation of Climate Normals. WMO, Geneva.

Zaytsev, O., Cervantes-Duarte, R., Montante, O., Gallegos-Garcia, A., 2003. Coastal upwelling activity of the Pacific shelf of Baja California Peninsula. J. Oceanogr. 59, 489—502. https://doi.org/10.1023/A:1025544700632